LBL-25779 c.2

Center for Advanced Materials

CAM

Presented at the 46th Annual Meeting of Electron Microscopy Society of America, Milwaukee, WI, August 7–12, 1988, and to be published in Ultramicroscopy

RECEIVED
LAWRENCE
BERKELEY LABORATORY

NOV 23 1988

LIBRARY AND
DOCUMENTS SECTION

Inversion Boundaries in GaAs Grown on Si

Z. Liliental-Weber, M.A. O'Keefe,
and J. Washburn

August 1988

TWO-WEEK LOAN COPY

This is a Library Circulating Copy
which may be borrowed for two weeks.

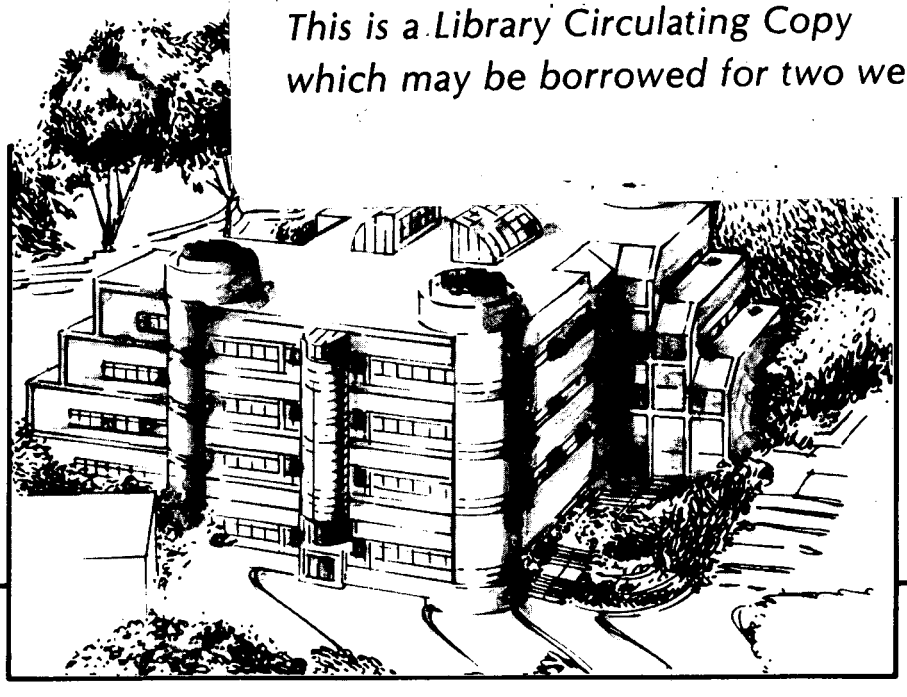

Materials and Chemical Sciences Division

Lawrence Berkeley Laboratory • University of California

ONE CYCLOTRON ROAD, BERKELEY, CA 94720 • (415) 486-4755

Prepared for the U.S. Department of Energy under Contract DE-AC03-76SF00098

LBL-25779 c.2

DISCLAIMER

This document was prepared as an account of work sponsored by the United States Government. While this document is believed to contain correct information, neither the United States Government nor any agency thereof, nor the Regents of the University of California, nor any of their employees, makes any warranty, express or implied, or assumes any legal responsibility for the accuracy, completeness, or usefulness of any information, apparatus, product, or process disclosed, or represents that its use would not infringe privately owned rights. Reference herein to any specific commercial product, process, or service by its trade name, trademark, manufacturer, or otherwise, does not necessarily constitute or imply its endorsement, recommendation, or favoring by the United States Government or any agency thereof, or the Regents of the University of California. The views and opinions of authors expressed herein do not necessarily state or reflect those of the United States Government or any agency thereof or the Regents of the University of California.

INVERSION BOUNDARIES IN GaAs GROWN ON Si

Zuzanna Liliental-Weber, * Michael A. O'Keefe,** and Jack Washburn*

*Center for Advanced Materials, **National Center for Electron Microscopy,

Lawrence Berkeley Laboratory, Berkeley, CA 94720

ABSTRACT

Inversion boundaries in GaAs grown on Si were investigated by high-resolution transmission electron microscopy. These boundaries were found to microscopically follow {110} planes, even when they appeared macroscopically along other planes, such as {111}. High resolution micrographs from edge-on {110} inversion boundaries were taken in [110] and [100] projection. In certain areas, shifts of the images of {111} and {200} planes across the boundaries were observed. Image simulations confirmed that the visibility of these shifts can only be observed for specific imaging conditions and within a limited range of sample thickness.

INTRODUCTION

Epitaxial growth of GaAs on Si substrates has recently drawn attention because of the potential to combining high-speed GaAs with well established Si technology [1-3]. There are three major materials problems which make perfect epitaxy difficult to achieve. The first is the large lattice mismatch, the second is the different thermal expansion coefficient, and the third is associated with growing a polar material on a non-polar substrate. The first two lead to misfit dislocations, stacking faults and the cracking of thick layers [4,5]. The third leads to the appearance of inversion boundaries commonly called antiphase boundaries (APBs) [6-8]. Across such boundary two As atoms or two Ga atoms are covalently bound instead of forming Ga-As bonds as in an ideal GaAs crystal. It is expected that APBs can result from the coalescence of GaAs domains independently nucleated on the Si substrate, when the coalescing domains have grown with one domain starting with a Ga layer and the other with an As layer. APBs might as well be nucleated, when the Si (100) surface contains single steps or an odd number of (a/4) Si steps. There are several reports in the literature that the growth of antiphase domains (APDs) can be successfully suppressed using Si substrate tilted by a few degrees from the exact (001) orientation [10,11]. However, the detailed mechanism of inversion boundary formation and their microstructure are not understood yet.

The presence of APDs can be determined chemically using molten KOH or photoelectrochemical etching [12,13]. Chemical etching gives however no information on the microscopic geometry of inversion boundary planes.

A very useful method for determining APDs in transmission electron microscopy is Convergent Beam Electron Diffraction (CBED) [9]. The coupling between the (200) reflection and the weak odd-index reflection in the Bragg position gives a special pattern (cross) in the (200) and (-200) discs that is sensitive to the order of the As and Ga planes in the samples [14,15]. However, this method does not allow us to see APBs on an atomic scale. Whether lattice imaging can be used to see more details has recently become a controversial issue. It was reported that a line of long dark spots and short bright spots can occur at the inversion boundary [16]. However, this line was observed neither by a 200CX TEM in GaAs samples grown on Si nor in multislice calculations for 200 KeV with a beam divergence half angle $1x10^{-3}$ rad for the samples up to 18nm thick [7].

In this paper we describe the results of lattice imaging of APBs performed with the Atomic Resolution Microscope (ARM,1MeV) in Berkeley.

EXPERIMENTAL

Our studies were carried out on GaAs grown by metal-organic chemical vapor deposition (MOCVD) on exactly oriented (001) Si wafers and by molecular-beam-epitaxy (MBE) on wafers tilted by 4° toward [110]. Cross-sectional samples along Si (110) and (100) were prepared for TEM observation with the conventional "sandwich" technique. Specimens were ion milled in order to obtain samples transparent to electrons. The samples were screened in a Philips 400 T (100KeV) TEM to obtain the CBED patterns to confirm the presence of APDs and then transferred to a JEOL JEM-200CX (200KeV) high resolution microscope or the ARM.

SIMULATION AND PROCESSING

Experimental images were analyzed by both, image simulation and processing techniques using the image-analysis facility at the National Center for Electron Microscopy (NCEM) [17].

Image simulations in the [110] projection were computed with the SHRLI programs [18] for a super cell of GaAs containing an inversion boundary. In this projection the primitive two-dimensional unit cell of GaAs has a size of 0.5652nm by 0.3996nm (i.e., a by $a/\sqrt{2}$). We chose a supercell consisting of one by ten unit cells of GaAs (0.5652nm by 3.9966nm) with the inversion boundary across the center of the cell. Images were simulated under ARM conditions at 1000 KeV for a multislice calculation of 400 slices which are 0.1nm thick, objective aperture size of 6.5 nm^{-1}, spherical abberation coefficient C_s of 2.8 mm, convergence semiangle of 0.6 miliradian, and spread of focus halfwidth of 10nm. Images were displayed on a Gould IP 9527 and printed on a Qume ScripTEN laser printer using 32 grey levels.

Experimental images were digitized into 2048 by 2048 pixels of eight-bit depth using an Eikonix digitizing camera, and processed using the SEMPER programs of Saxton et al. [19] on a uVAX microcomputer, displayed on the IP 9527, and printed on the ScripTEN.

RESULTS AND DISCUSSION

In both the MOCVD grown and the MBE grown samples a high density of defects were observed in cross-sectioned samples. These defects consisted mostly of stacking faults and dislocations. APDs were determined in both samples by CBED. Generally, two types of APBs were observed: those which propagated to the surface of the GaAs epilayer (see [9], Figs. 1-3) and those which were annihilated inside the epilayer (see [9], Fig. 5). Both types of APBs were highly faceted, especially in the area close to the interface. APBs which were annihilated changed their boundary plane from place to place, forming nearly half-spherical APDs inside the epilayer. Near the sample surfaces, straight

APBs on {110} planes can be observed. Some APBs appear macroscopically to fall on {111} planes. Microscopically these APBs are found to be staircase-like, composed of small regions of {110} boundaries viewed either edge-on or visible as ribbons, if they were inclined to the surface (see [9], Fig. 3). This faceting on the (110) planes is probably driven by the minimalization of interfacial energy, in agreement with Petroff's prediction [20] that the {110} APBs have the lowest interfacial energy. The appearance of APBs on staircases along {111} planes might be connected with the growth front and the three-dimensional growth on highly packed {111} planes. At some places, dislocations were found along the intersection of two {110} APBs tilted 60° to each other (Fig. 1). It is not possible to determine if their presence initiated the switching to another {110} plane or if APB intersections act as dislocation "sinks." On some CBED patterns a slight tilt (in the range of 1° or less) can be observed. This may suggest that APBs are formed when two independently growing islands meet each other. Thus APBs in GaAs on Si can have a superposition of "wrong" bonding and local tilting (local low angle boundaries), which can lead to the formation of additional dislocations (Fig. 2). It was frequently noticed that APBs are very efficient obstacles to the propagation of defects (see [9], Fig. 4). The ideal way to prevent defect propagation toward the surface of the GaAs epilayer would be to introduce APBs parallel to the interface with Si.

High resolution micrographs from edge-on parts of {110} APBs show often a lattice image shift on both sides of the boundary (Fig. 3). The shift is more visible if the rows of dots in the micrograph are extrapolated toward the boundary from more than 1nm away because some areas along the boundary have a distortion in the lattice image caused by strain or by a drastic change in thickness on both sides of the antiphase boundary. In the [110] projection this shift can be seen on both {111} planes and the {200} planes. Looking along the {200} planes the image shift is 0.14nm. Such a step of 0.14nm along {200} planes across the APB was as well observed in [100] projection (Fig. 4). There also were areas where the visibility of APBs disappeared and the boundary could not be recognized from the lattice image, as it was observed by Kuan [7].

To understand the lattice image visibility of the inversion boundary simulated images were computed in the [110] orientation for the ARM conditions for crystal thicknesses up to 40 nm over a defocus range from -10 nm to -100 nm. The model containing a {110} APB is shown in Fig. 5. In [110] projection the pairs of Ga and As atoms are seperated by 0.14nm and usually imaged only as one dot. Our simulations show, that under the image conditions described above the black dots correspond to the location of the As atoms rather than to the center of the As-Ga pairs. This effect enables to observe a shift of the {111} and {200} planes across a {110} APB. Examination of the simulated images showed that the image shift at the inversion boundary is only visible over a limited range of thickness [21] centered on 24 nm and extending 3 nm to each side of this thickness (Fig. 6a-h). Within the range of defocus considered, the variation in defocus did not destroy the visibility (Fig. 6i-l). It should be remembered that the optimum thickness of 24 nm found here is specific to the accelerating voltage (1MeV) and imaging conditions used, and may be different for other electron microscopes.

To investigate whether the APBs were initiated at a single step on the Si surface, high resolution micrographs were taken in the [100] projection. However, it was not clear from Fig. 4 if a single step was present at the interface or if the inversion boundary formation was initiated because of the presence of an amorphous contamination layer at the interface. This amorphous band is not believed to be an artifact due to TEM sample preparation. Based on the experience on metal/GaAs interfaces an amorphous band was observed only when impurities were present at the interface [22].

Experimental images of GaAs on Si in [100] orientation were processed to try to discover any feature of the Si surface that might be associated with the inversion boundary observed in the GaAs. An image of 512 by 512 pixels containing the Si/GaAs interface at the inversion boundary was extracted from a 2048 by 2048 digitized image. In order to try to increase the visibility of the image region where the inversion boundary approached the interface, this image was Fourier transformed (Fig. 7a) and a series of windows of 0.3 of the reciprocal lattice parameter was applied to the resulting diffractogram

(Fig. 7b) before back transformation was made to the real space (Fig. 7c). From the processed image one can conclude that an a/4 single step was present on the Si surface in the area of the inversion boundary considered. In addition, it was very clear from the processed image that the Si surface was very wavy, and one can conclude that additional inversion boundaries were formed, that annihilated within the first few monolayers of the GaAs near the interface with Si.

CONCLUSIONS

Antiphase boundaries which were annihilated within the GaAs epilayer and APBs which propagated to the GaAs surface were observed in the GaAs grown by both MOCVD on exactly (001) oriented Si substrates and by MBE on 4° off (001) Si substrates. The annihilated APBs were found to change the boundary planes from area to area forming nearly half-spherical APDs inside the layer adjacent to the interface. The APBs which propagated to the surface followed mostly {110} planes. High resolution micrographs from edge-on {110} inversion boundaries were taken in [110] and [100] projection. A shift of the lattice image of 0.14nm along {200} planes was observed in some areas of the boundaries. It was confirmed by image simulation that the visibility of this shift is limited to the sample thickness of 24 ± 3 nm for a 1 MeV accelerating voltage. The image processing of the lattice image micrograph of the GaAs/Si interface in [100] projection allows one to conclude that a/4 single steps were present at the Si surface to initiate the inversion boundary formation. A few monolayers at the interface were very wavy and the presence of annihilated inversion boundaries very close to the Si substrate can be considered.

This study shows, that it is possible to identify inversion boundaries by high-resolution electron microscopy combined with image simulation. However, this identification is very critically dependent on the imaging conditions. The unambigous determination of antiphase domains requires the use of convergent beam electron diffraction [15].

ACKNOWLEDGEMENTS

The authors gratefully acknowledge fruitful discussions with E.R. Weber and U. Dahmen. This work was supported by the Director, Office of Energy Research, Office of Basic Energy Sciences, Materials Science Division of the U.S. Department of Energy under Contract No. DE-ACO3-76SF00098. The use of the facilities in the National Center for Electron Microscopy in Berkeley is greatly appreciated.

REFERENCES

[1] "Heteroepitaxy on Silicon," Eds. J.C.C. Fan and J.M. Poate, *Mat. Res. Soc. Symp. Proc.* vol. **67** (1986).

[2] "Heteroepitaxy on Silicon II," Eds. J.C.C. Fan, J.M. Phillips and B.Y. Tsaur, *Mat. Res. Soc. Symp. Proc.* vol. **91** (1987).

[3] "Initial Stages of Epitaxial Growth," Eds. R. Hull, J.M. Gibson and D.A. Smith, *Mat. Res. Soc. Symp. Proc.* vol. **94** (1987).

[4] N. Otsuka, C. Choi, Y. Nakamura, S. Nagakuva, F. Fischer, C.K. Peng, and H. Morkoc, *Mat. Res. Soc. Symp. Proc.*vol. **67** (1986), p. 85.

[5] Z. Liliental-Weber, E.R. Weber, J. Washburn, T.Y. Liu, and H. Kroemer, *Mat. Res. Soc. Symp. Proc.*vol. **91** (1987), p. 91.

[6] H. Kroemer, *Mat. Res. Soc. Symp. Proc.* vol. **67** (1986), p. 3.

[7] T.S. Kuan and C.A. Chang, *J. Appl. Phys.***54** (1983) 4408.

[8] N.H. Cho, B.C. DeCooman, C.B. Carter, R. Fletcher, and D.K. Wagner, *Appl. Phys. Lett.* **47** (1985) 879.

[9] Z. Liliental-Weber, E.R. Weber, L. Parechanian-Allen, and J. Washburn, *Ultramicroscopy* (1988), in print.

[10] D.E. Aspen and J. Ihm, *Mat. Res. Soc. Symp. Proc.* vol. **91** (1987), p. 45.

[11] M. Kawabe and T. Ueda, *Jap. J. Appl. Phys.* **26** (1987) L944.

[12] K. Morizane, *J. Cryst. Growth* **38** (1986) 249.

[13] H. Noge, H. Kano, M. Hashimoto, and T. Igarashi, *J. Appl. Phys.* .. (1988) .

[14] J. Taftø and J.C. Spence, *J. Appl. Cryst.* **15** (1982) 60.

[15] Z. Liliental-Weber and L. Parechanian-Allen, *Appl. Phys. Lett.* **49** (1986) 1190.

[16] C.B. Carter, N.H. Cho, S. McKernan, and D.K. Wagner, *Mat. Res. Soc. Symp. Proc.* vol. **91** (1987), p. 181.

[17] M.A. O'Keefe, *Proc. 45th Ann. EMSA Meetg.*(1987), p. 364.

[18] M.A. O'Keefe and P.R. Busek, *Trans. Amer. Cryst. Assoc.***15** (1979) 27.

[19] W.O. Saxton, T.J. Pitt, and M. Horner, *Ultramicroscopy* **4** (1979) 343.

[20] P.M. Petroff, *J. Vac. Sci. Techn.* **B4** (1986) 874.

[21] Z. Liliental-Weber, M.A. O'Keefe, and J. Washburn, *Proc. 46th Ann. EMSA Meeting* (1988), in print.

[22] Z. Liliental-Weber, J. Washburn, N. Newman, W.E. Spicer, and E.R. Weber, *Appl. Phys. Lett.***49** (1986) 1514.

FIGURE CAPTIONS

Figure 1: Disocations present at the intersection of different planes of antiphase boundaries.

Figure 2: Dislocation (large arrow) present at a straight section of an {110} antiphase boundary (indicated by small arrows). In contrast to the other high-resolution micrographs, this picture was taken in a JEOL 200 CX TEM.

Figure 3: High resolution image of a {110} APB in [110] projection. Note the 0.14nm shift along the (200) planes across the boundary, as shown by two arrows.

Figure 4:

a) [100] projection of two antiphase boundaries in MOCVD GaAs/Si marked by arrows, one propagating to the surface and one annihilated inside the GaAs layer. Note the contrast near the GaAs/Si interface, which indicates the presence of additional, small antiphase domains.

b) High magnification micrograph from the interfacial area marked in Fig. 4a. Note the contamination layer present at the interface and the 0.14nm shift along the (200) planes across the boundary. The arrow indicates the region used for the image processing shown in Fig. 7.

Figure 5: Model showing the atom arrangement at an {110} antiphase boundary. The supercell used for the image simulations is outlined by the rectangle.

Figure 6: Simulated images calculated for the ARM (1MeV) from an edge-on {110} inversion boundary in GaAs for defocus Δf = -50nm and different sample thicknesses t:

a) t = 8nm, b) t = 16nm, c) t = 20nm, d) t = 22nm, e) t = 24nm, f) t = 26nm, g) t = 32nm, and h) t = 40nm.

For a sample thickness t = 24nm the images were calculated with the defocus values: i) Δf = -30nm, j) Δf = -50nm, k) Δf = -70nm, l) Δf = -90nm.

Figure 7:

a) Fourier transformed image (computed diffractogram) of the digitized image indicated in Fig. 4b.

b) Computed diffractogram after application of windows of 0.3 reciprocal lattice parameter.

c) Processed image obtained after reverse Fourier transformation of the diffractogram in Fig. 7b. This image shows clearly an a/4 single step at the GaAs/Si interface at the origin of the antiphase boundary. The Si surface appears to be quite uneven.

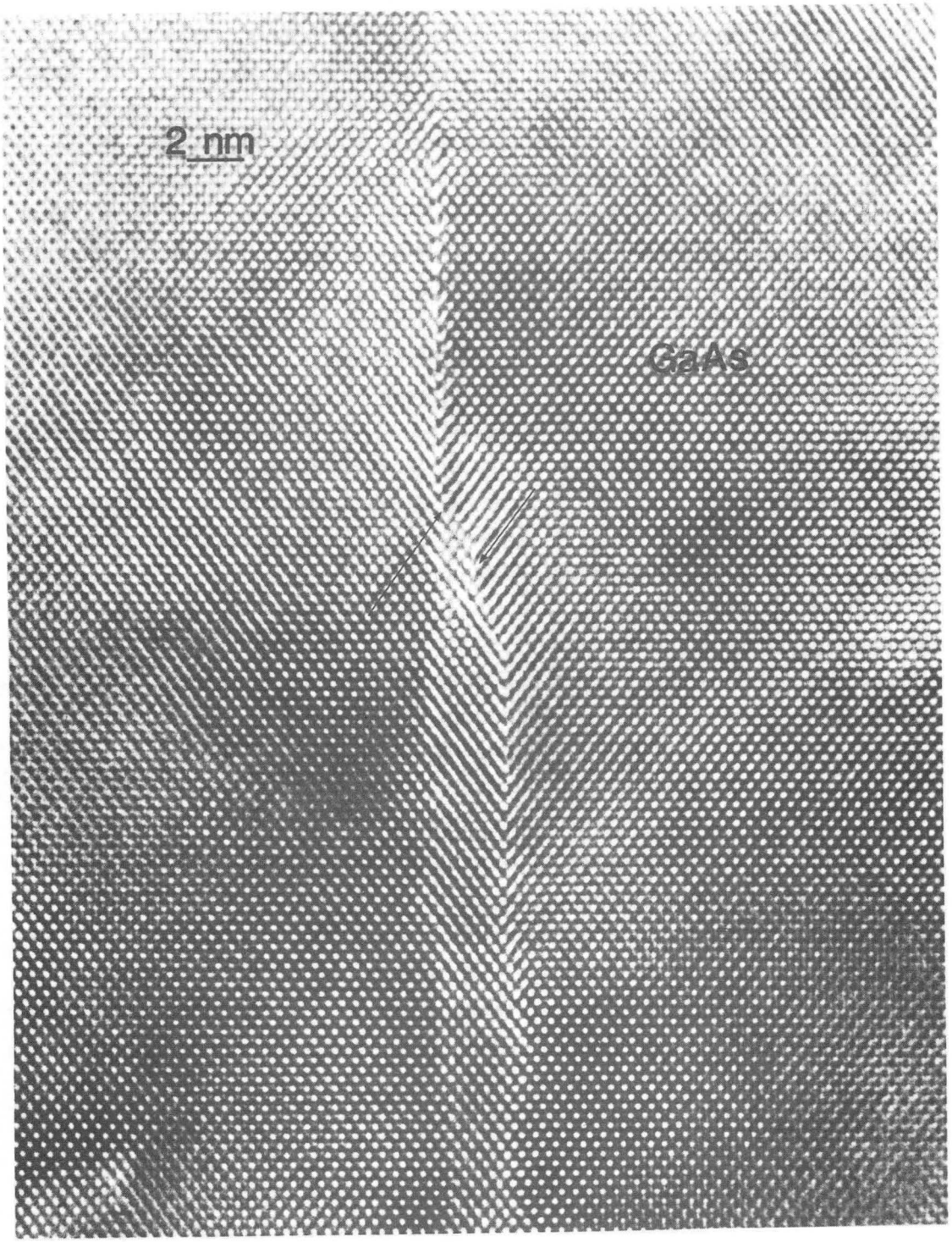

Fig. 1

XBB 887-7289

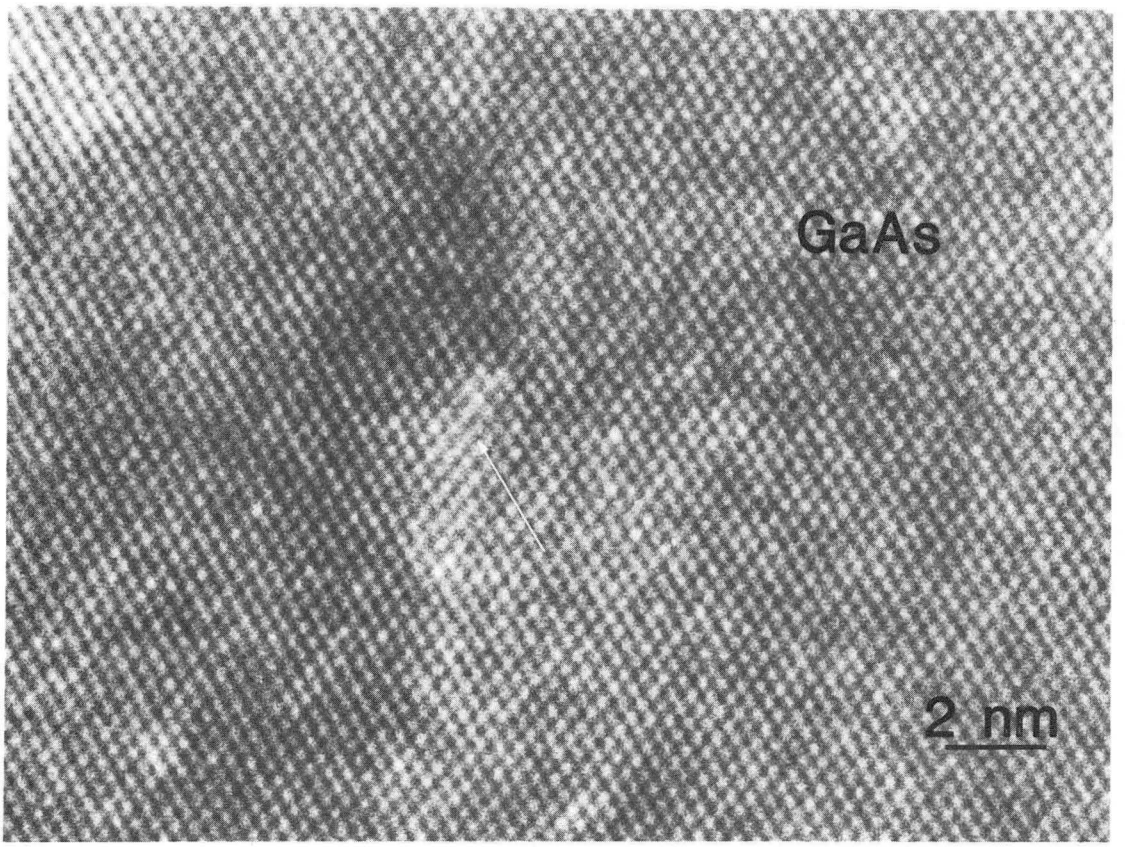

Fig. 2 XBB 887-7288

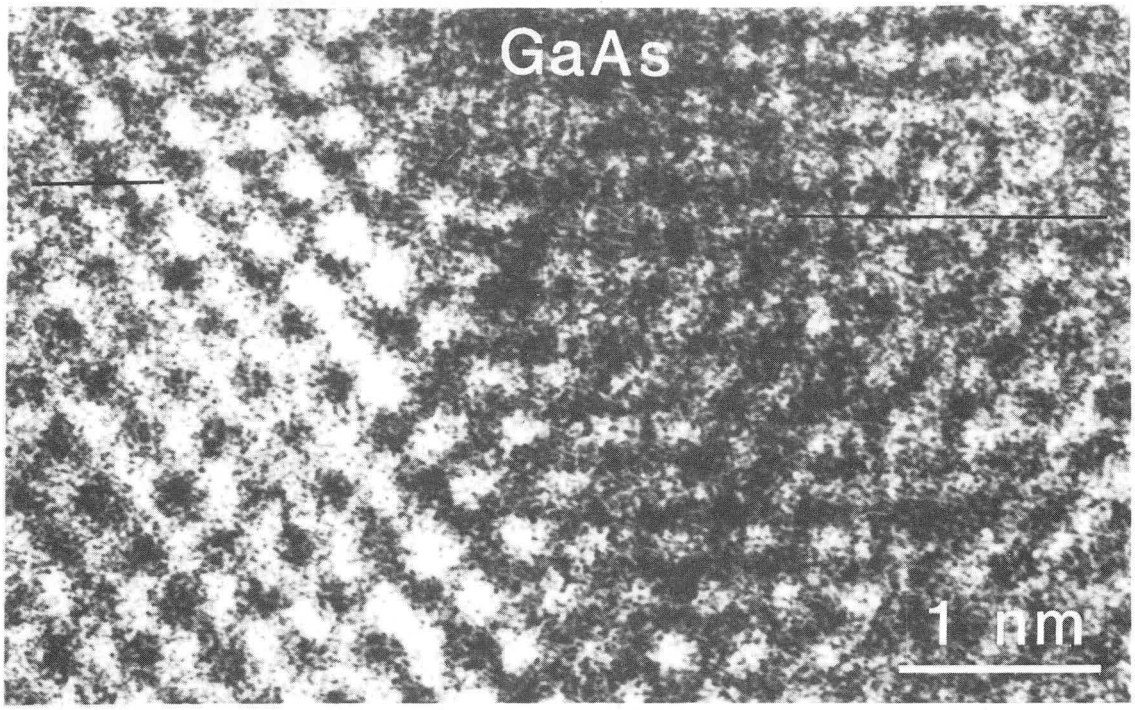

Fig. 3 XBB 888-7334

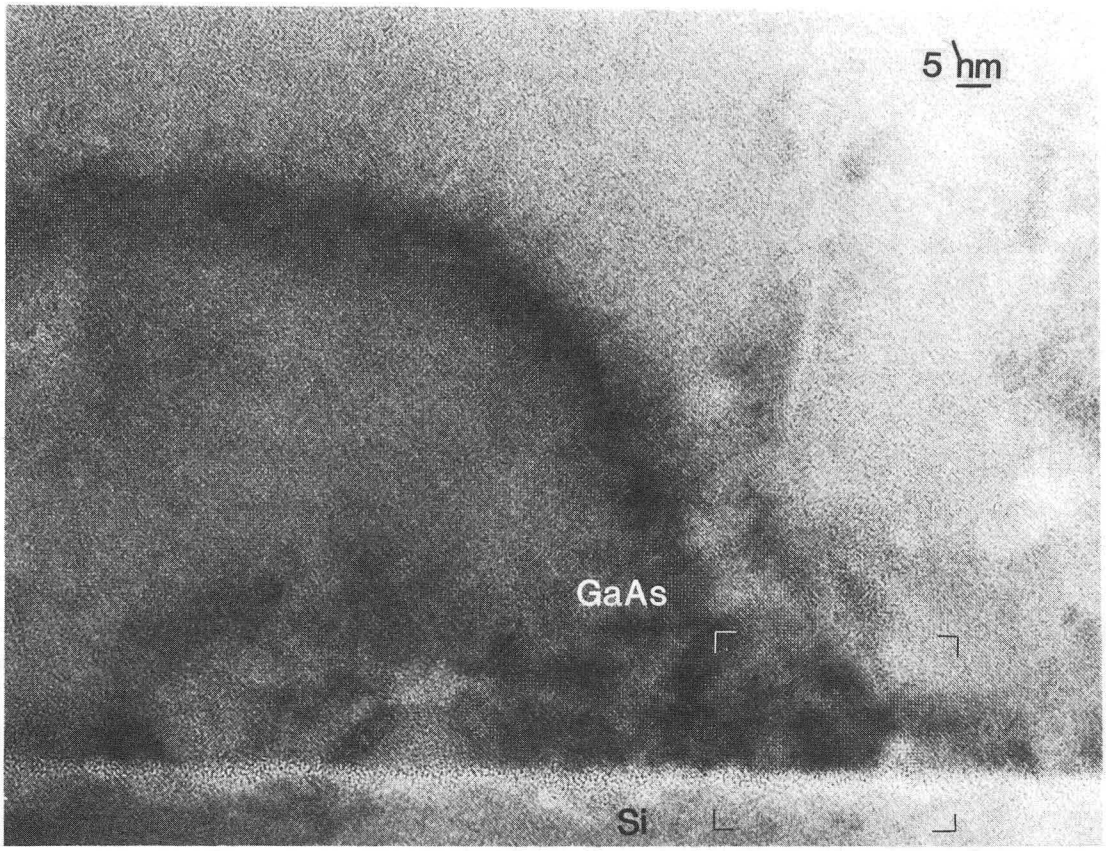

Fig. 4a XBB 887-7290

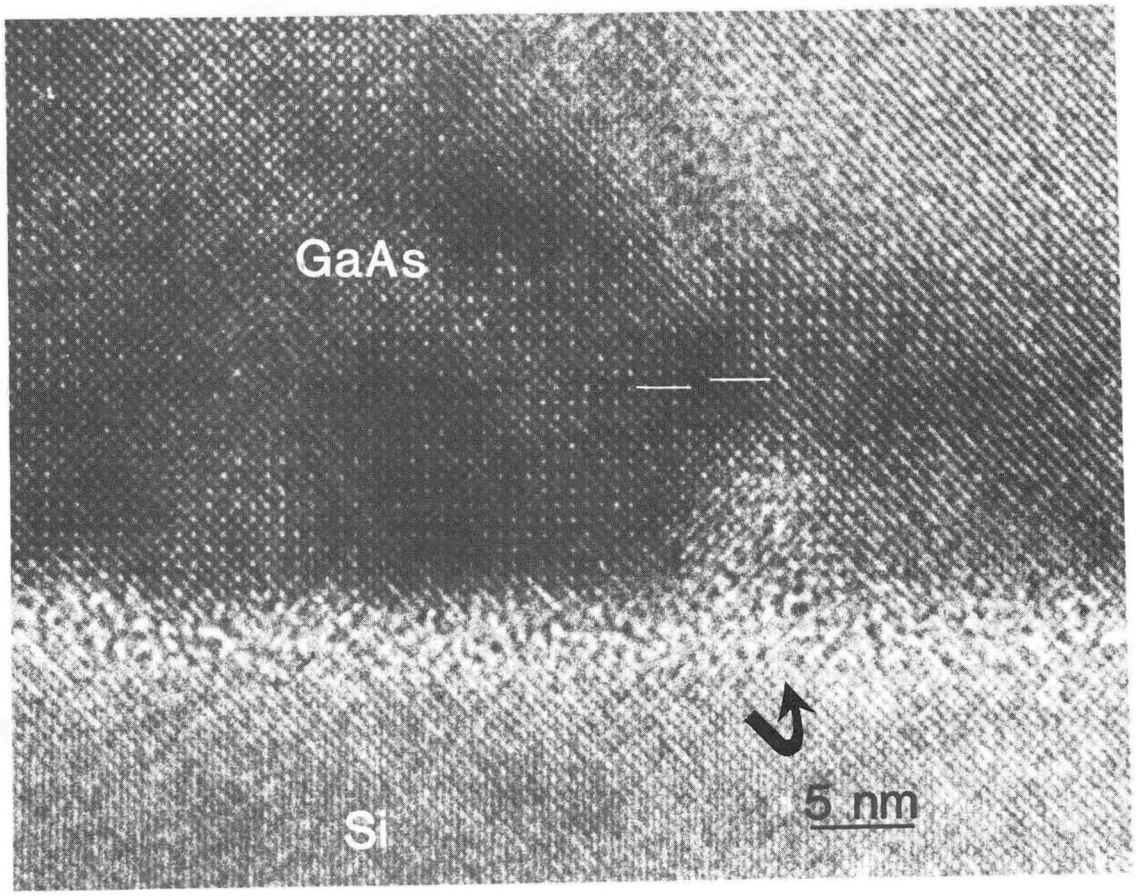

Fig. 4b

XBB 887-7287

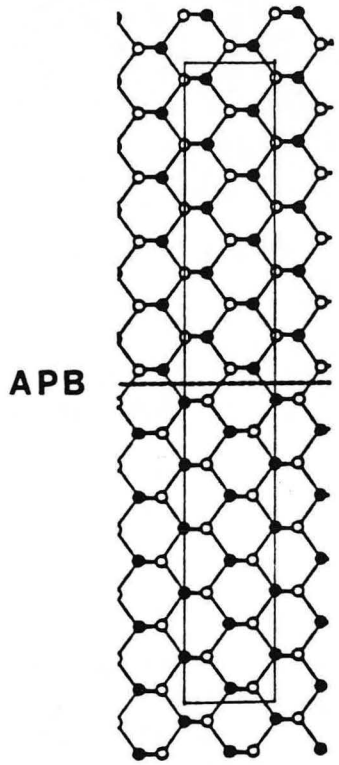

Fig. 5 XBB 888-7411 (bottom)

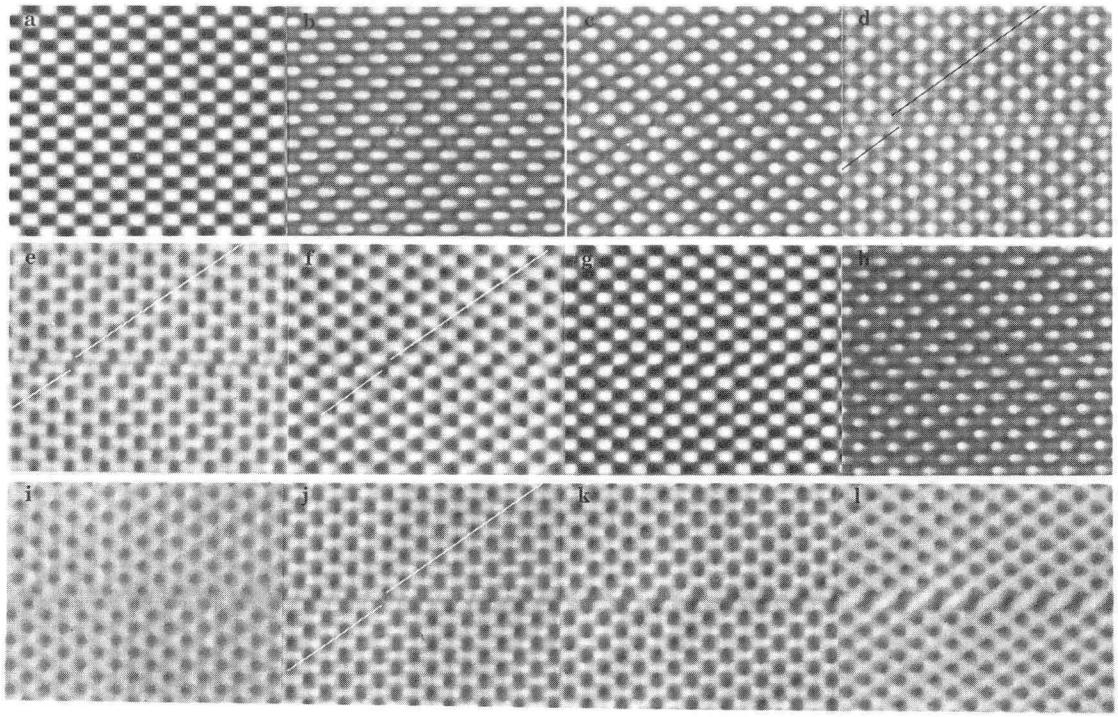

Simulated images calculated for the ARM-1MeV from edge-on inversion boundary in GaAs for defocus=-50 nm from different sample thickness: a) = 8 nm, b) = 16 nm, c = 20 nm, d) = 22 nm, e) = 24 nm, f) =26nm, g) = 32 nm, h) = 40 nm;
i-l): Images for the thickness = 24 nm with defocus of -30 nm, -50 nm, -70 nm and -90 nm.

Fig. 6 XBB 888-7410

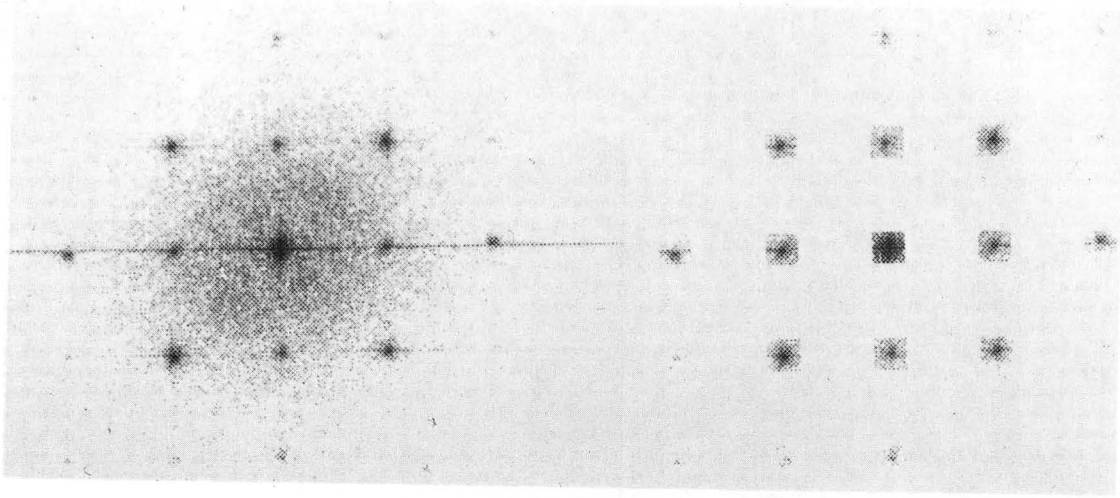

Fig. 7 a,b

XBB 888-7411 (top)

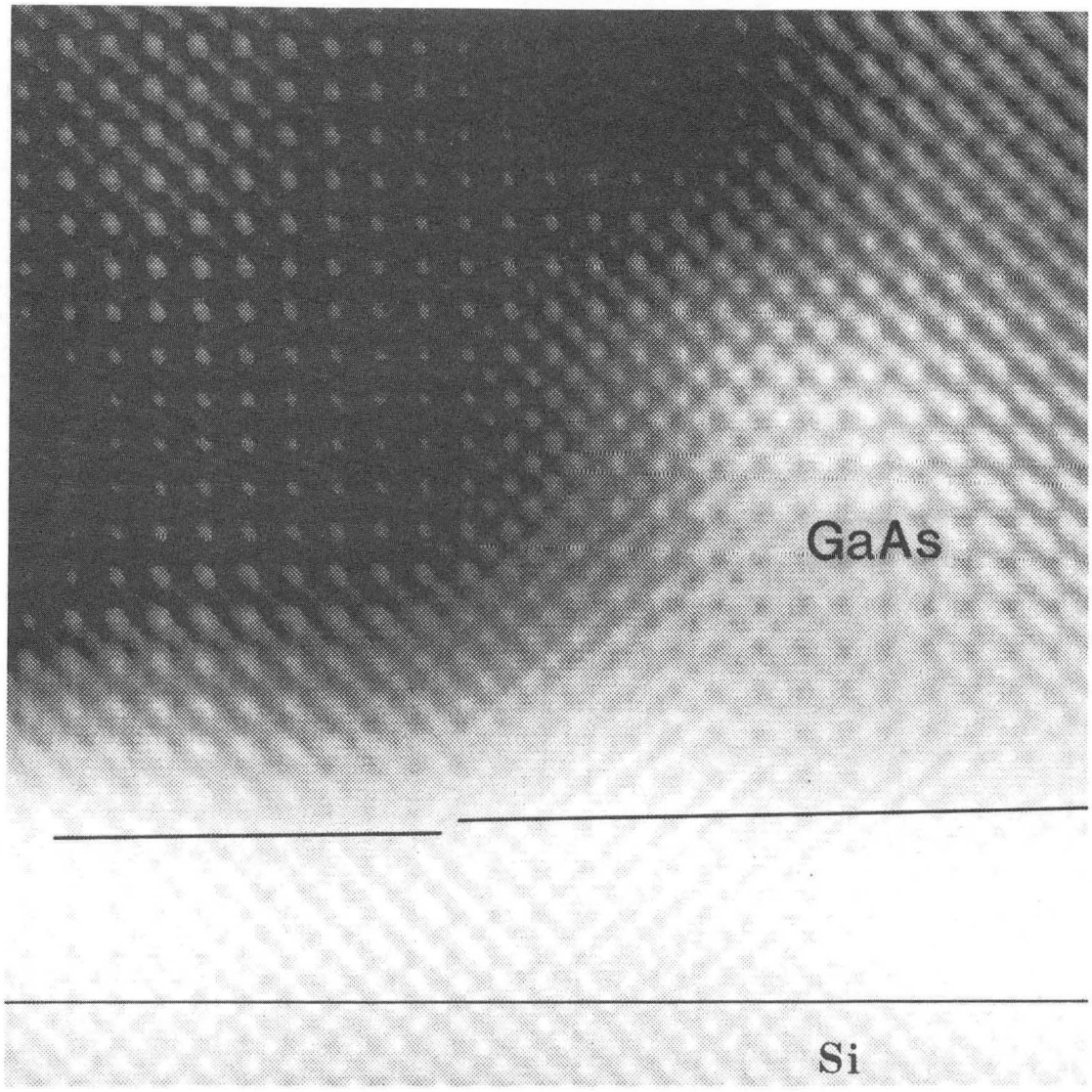

Fig. 7c XBB 888-7412

LAWRENCE BERKELEY LABORATORY
TECHNICAL INFORMATION DEPARTMENT
UNIVERSITY OF CALIFORNIA
BERKELEY, CALIFORNIA 94720